Supporting Information

Ullrich-Lüter et al. 10.1073/pnas.1018495108

SI Materials and Methods

Animal Supply and Culture. ***Strongylocentrotus purpuratus.*** Adult animals were collected from a location at 25 to 30-m depth in the San Diego, CA bay, maintained for a week in an open tank system at the Kerchoff Marine Laboratory, Corona Del Mar, CA, shipped to Naples, Italy, by Global Animal Transport, and subsequently housed in circulating seawater aquaria at the Stazione Zoologica Anton Dohrn, Naples, Italy, 15 °C, under a day/night light cycle. Larvae were cultured according to standard procedures (1) at 15 °C, in filtered seawater diluted 9:1 with deionized water, and fed with *Isochrysis galbana* maintained at 3,000 cells/mL.

Asterias rubens. Spawning was induced by intracoelomic injection with 2 mL of 0.1 mM 1-methyladenine. Fertilized eggs were rinsed in filtered seawater and at the two-cell stage were transferred to 5 L aquaria at a density of 10 embryos per milliliter. Cultures were maintained at constant temperature (12 °C), a salinity of 32‰ and alkalinity of 2.12 ± 0.02 mM. After day 2, larvae were fed daily with the red alga *Rhodomonas lens* at a concentration of 50 to 200 μg of carbon per liter.

Phototaxis Experiments. Adult animals were dark-adapted for 10 min in the center of a 10 × 50-cm glass tank, filled with seawater to a depth of 6 to 7 cm. The tank was externally obscured with black adhesive foil except for a window of 1 × 5 cm, located at the center of each short side of the tank. Phototaxis experiments were performed using a goose neck (1-cm diameter) optic fiber light source (color temperature 3,350 K, CRI 100Ra8) (see white spectrum 1 in Fig S1*D*) placed 1 cm next to the shorter side of the tank at the center of the transparent window. Twenty adult *S. purpuratus* were included in the test series. Controls included 20 adult animals kept under dark adaptation conditions for a period of 30 min. These animals did not display any substantial movements within the control period. Animal behavior in light conditions was recorded using a tripod fixed digital camera and the speed at which they moved away from the directional light was calculated by measuring length spanning from start to end position of the animal's body center over each period. Experiments on juveniles used the same apparatus except that tank dimensions were 2.5 × 20 cm. About 50 specimens of *S. purpuratus* and *Paracentrotus lividus*, aged from 0 to 1 mo after metamorphosis, were tested individually and subsequently fixed for immunostaining.

The same 10 × 50-cm tank, equipped with an LED-based light system of variable intensity (M2M Engineering), was used to measure *S. purpuratus* adult phototaxis at different wavelengths in comparison with white light (for the set up used, see Fig. S1 *A* and *B*, and white spectrum 2 in Fig. S1*D*). A total of 15 to 20 animals (6- to 8-cm diameter), randomly picked in groups of 10 and adapted for 1 h in a 20 × 50-cm tank (in seawater communication with the 10 × 50-cm tank), at 15 °C, in dark conditions, were used for the whole experiment. For each measurement, an animal was taken from the 20 × 50-cm tank, placed in the center of the 10 × 50-cm tank, blocked by a dark box (9 × 9 cm) (Fig S1*A*), and allowed to rest in the dark box for 1 min. After this resting period, light was turned on, the box was removed, and the animal was observed for 2 min. The distance span by the animal from start to end position over the 2-min period was measured using a ruler placed at the bottom of the tank (Fig. S1*B*). Light intensity in seawater at the different sea urchin positions was measured for each monochromatic and white light and was found to be ranging between 0.2 and 1.0 μwatt/cm^2 throughout the experiment.

In Situ Hybridization. Fragments of *Sp-opsin4* and *Sp-Pax6* were amplified from genomic DNA by PCR using specific primers (Op4IL: ATGCCATCTTCTGGTCCATC/Op4IR: AGCAGAAGCAGAAGCAGGAG; SpPax6F: AGAGGCCGAAGAAGGAGAAG/SpPax6R: CGGACTCTACCCGACAGAAG). PCR products were purified and cloned into pCRII-TOPO vector (Invitrogen) according to the manufacturer's instructions, and the identity of the inserts was determined by sequencing. Whole-mount in situ hybridizations (WMISH) were performed as described by Arendt et al. (2). For fluorescent WMISH, the staining protocol outlined by Cole et al. (3) was followed and signal was developed with Cy3-fluorophore-conjugated tyramide (Perkin-Elmer). Accuracy of the WMISH results was confirmed by control experiments using sense probes. Both antisense- and sense-digoxigenin–labeled RNA probes were obtained using a DIG-RNA labeling kit (Roche), following the manufacturer's instructions by using 1 μg of linearized plasmids. RNA probes were purified using the Mini Quick Spin RNA Columns (Roche). After staining, samples were mounted in glycerol and analyzed on a Zeiss Axio Imager M1 microscope operating in differential interference contrast mode or a Zeiss 510Meta or a Leica SP5 confocal microscope.

Antibody Production and Purification. Purified polyclonal antibodies against the c-terminal tail of Sp-Opsin4 were developed upon request by PRIMM (www.primm.it). Recombinant proteins were produced as His-Tag fusions.

Immunohistochemistry. Tissues and specimens were fixed in 4% paraformaldehyde in filtered seawater at room temperature for 15 min, then postfixed with ice-cold methanol for 1 min. Fixed specimens were rinsed in PBS pH 7.4 and then blocked 4% BSA containing 0.1% Tween-20 at room temperature. Anti-synaptotagmin B (1E11) (4), anti-acetylated tubulin (Sigma), and anti–Sp-Opsin-4 were diluted 1:200, 1:250, or 1:50, respectively, in PBS. After an overnight incubation (at room temperature), embryos were rinsed in PBS and then incubated in a 1:1,000 dilution of Alexa488 conjugated anti-rabbit IgG and Alexa568 conjugated anti-mouse IgG (Molecular Probes) for 2 h at room temperature. After several washes in PBS, specimens were examined using a Leica SP 5 or Zeiss 510Meta confocal laser-scanning microscope. Pictures shown were produced by recording confocal image stacks and projecting them in the *z* axis using MacBiophotonics ImageJ or the Leica SP 5 software. Colocalization of Sp-Opsin4 protein and *Sp-opsin4* RNA was performed with the colocalization tool of MacBiophotonics ImageJ. Projection of Sp-Opsin4–positive photoreceptor cells (PRCs) onto scanning electron microscopy (SEM) pictures was obtained using Photoshop CS2 clipping function. Decalcification of dissected adult tissues including parts of the test was obtained by treatment with 2% ascorbic acid/0.15 M NaCl for 3 d on a slow rotator at room temperature. Immunohistochemistry coupled to WMISH was similarly performed by incubating anti-acetylated tubulin and anti–Sp-Opsin-4 antibodies together with the anti–digoxigenin-11-UTP antibody. After WMISH staining, specimens were rinsed in PBS and then incubated in a 1:1,000 dilution of Alexa488 conjugated anti-rabbit IgG and Alexa633 conjugated anti-mouse IgG (Molecular Probes) and washed as described previously.

Scanning Electron Microscopy. Specimens were fixed in 2.5% glutaraldehyde in PBS and rinsed in PBS several times. After postfixation in 1% Os_4O in PBS, specimens were dehydrated in a graded acetone series, transferred to 100% Ethanol, and dried

using a critical point dryer. After mounting on stubs, they were sputter coated with gold and viewed on a REM Quanta SEM.

μCT Scanning. A small (approximately 3 × 5 mm) part of the skeleton of an adult specimen of *S. purpuratus* was scanned using a Phoenix nanotom μCT scanner. The system uses a tungsten X-ray source and a CCD camera with a 2,304 × 2,304-pixel matrix. Scanning was accomplished using 1,440 images at 360° rotation, resulting in a voxel size of 5.5 μm. Scanning parameters were: 150 kV, 180 μA, 750-ms exposure time, and three averages. Image reconstruction was performed using the software provided with the μCT system. Three-dimensional visualization was accomplished using VGStudioMAX 2.0.

Transmission Electron Microscopy, Including Immunogold Labeling. Specimens were fixed in 2.5% Glutaraldehyde in PBS and rinsed in PBS several times. After postfixation in 1% Os_4O in PBS, specimens were dehydrated in a graded acetone series and embedded in plastic resin (Araldite M, Fluka; art. no.: 10951) for 48 h at 60 °C. Serial sections were cut using a diamond knife and a Reichert ultramicrotome S and stained with uranyl acetate and lead citrate (Phoenix ultrastain, Staining Technologies). Examination was carried out on a Phillips CM Biotwin transmission electron microscope (TEM). Three-dimensional reconstruction of PRCs and surrounding tissues was performed using Photoshop CS2 for alignement of the TEM serial section photographs and Amira 2.0 for subsequent 3D surface rendering.

For immunogold labeling on ultrasections, *S. purpuratus* tube feet were fixed in 0.5% glutaraldehyde/4% PFA in PBS, pH7.4 initially and then decalcified in 1% ascorbic acid/0.15 M NaCl on ice. Dehydration and embedding in LR White medium followed the protocol of Agar Scientific Limited; polymerization was carried out in fully filled small Eppendorf tubes within an UV-incubator for 48 h at room temperature. Obtained sections (see above) were mounted on nickel grids and then processed following the protocol of Tan et al. (5), including treatment with ammonium chloride and blocking with 5% normal goat serum/0.1% BSA. Primary antibody incubation (anti–Sp-Opsin4) 1:50 in PBS overnight was followed by incubation with anti-rabbit IgG Gold (Sigma Aldrich; Cat. No.: G7402) for 2.5 h, at room temperature. Gold enhancement was performed using the Nanoprobes GoldenhanceTM-EM kit, following the manufacturers instructions, except that no postfixation step was applied.

1. Leahy PS (1986) Laboratory culture of *Strongylocentrotus purpuratus* adults, embryos, and larvae. *Methods Cell Biol* 27:1–13.
2. Arendt D, Tessmar-Raible K, Snyman H, Dorresteijn AW, Wittbrodt J (2004) Ciliary photoreceptors with a vertebrate-type opsin in an invertebrate brain. *Science* 306: 869–871.
3. Cole AG, Rizzo F, Martinez P, Fernandez-Serra M, Arnone MI (2009) Two ParaHox genes, *SpLox* and *SpCdx*, interact to partition the posterior endoderm in the formation of a functional gut. *Development* 136:541–549.
4. Nakajima Y, Kaneko H, Murray G, Burke RD (2004) Divergent patterns of neural development in larval echinoids and asteroids. *Evol Dev* 6:95–104.
5. Tan E, et al. (2001) The relationship between opsin overexpression and photoreceptor degeneration. *Invest Ophthalmol Vis Sci* 42:589–600.

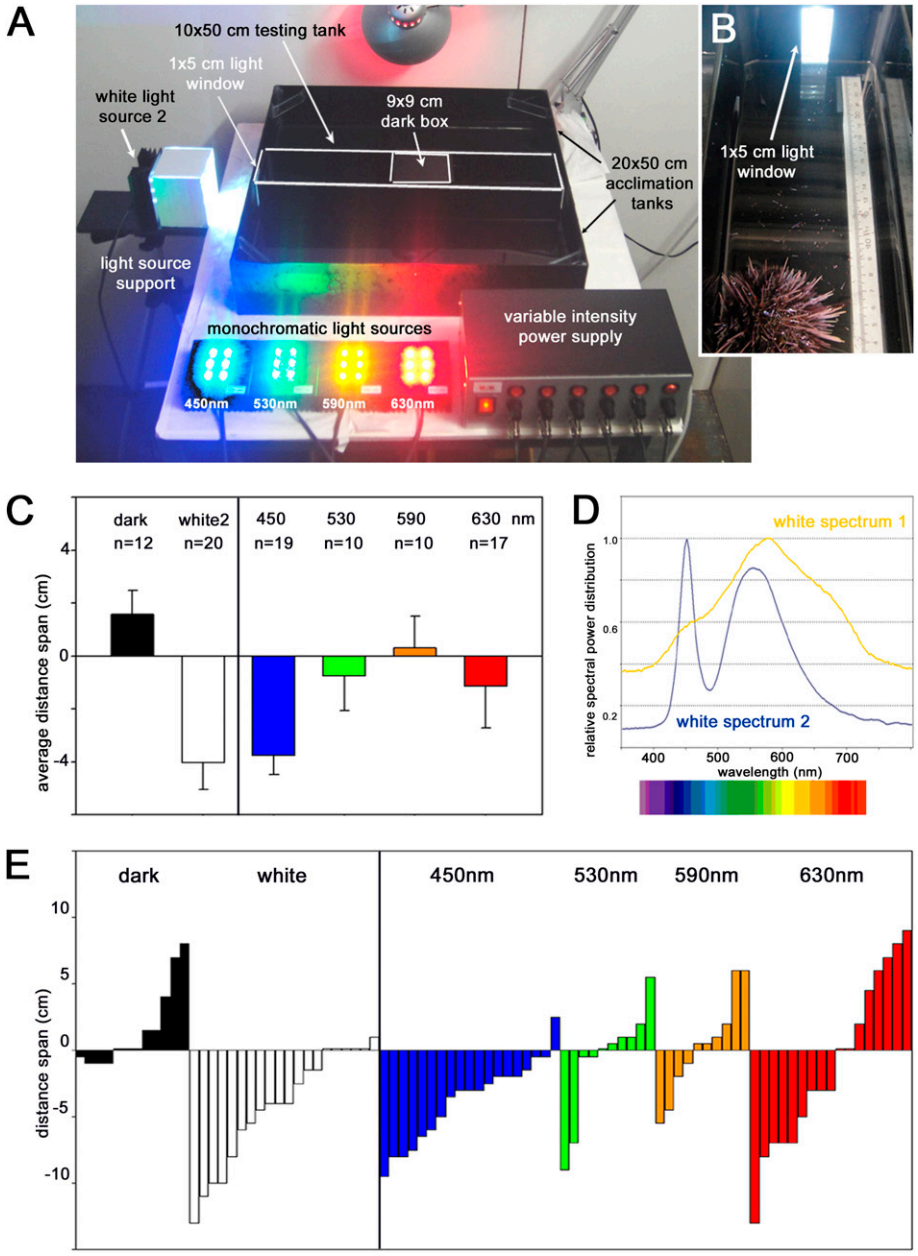

Fig. S1. Adult *S. purpuratus* phototaxis. (*A*) Set up of tanks and LED-based light sources used. (*B*) Detail of 10 × 50-cm testing tank with ruler at the bottom. (*C*) Bar graph of average distance span as calculated from *E* for each different light condition. SD is shown for each bar. (*D*) Full light spectra measured for the white-light sources used in this work. (*E*) Measured distance span for each sea urchin tested in different light conditions (see *SI Materials and Methods* for details). Measured distances were taken as positive (+) or negative (–) depending upon whether the sea urchin was moving toward or away from the light source. Plus and minus where arbitrarily set for the measurements in dark conditions.

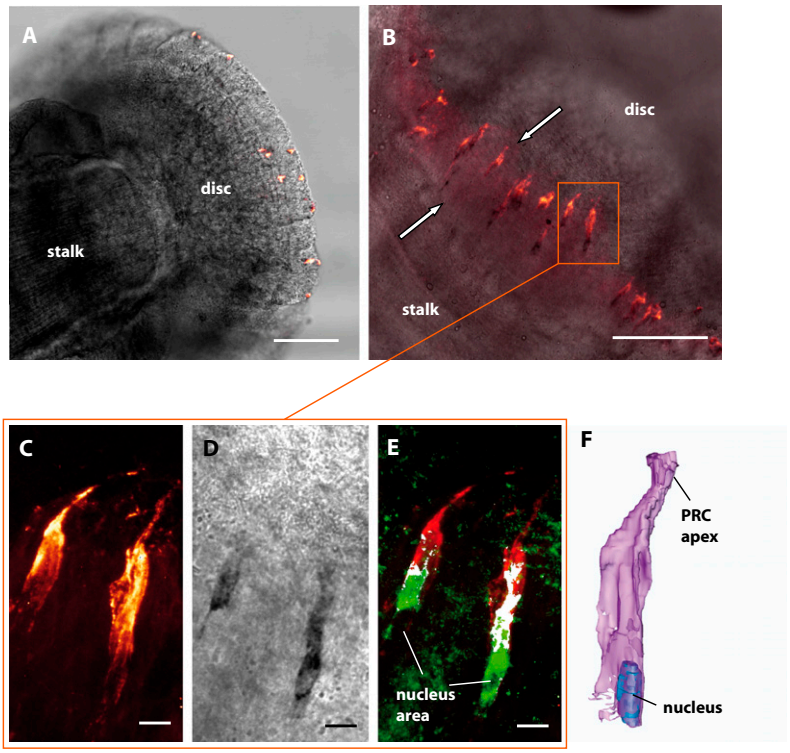

Fig. S2. Double localization of Sp-Opsin4 protein and *Sp-opsin4* RNA. (*A*) Confocal *z*-projection of tube foot whole mount with *Sp-opsin4* RNA (black) localized by in situ hybridization and Sp-Opsin4 protein (hot red) stained by antibody labeling. (*B*) Same specimen, *z*-projection of higher magnification of the rim of the disk (indicated by white arrows), showing several PRCs. (*C*) A *z*-projection of Sp-Opsin4 immunostaining, selected cells from *B*. (*D*) A *z*-projection view of the same cells, recorded in transmission mode showing *Sp-opsin4* RNA labeling by NBT/BCIP (black). (*E*) Colocalization of Sp-Opsin4 protein and RNA in the middle part of the receptor cell (Colocalization tool, MacBiophotonics ImageJ; see *SI Materials and Methods*). (*F*) Schematic reconstruction (for details see *SI Materials and Methods*) of Sp-Opsin4–positive PRC from TEM serial sections showing the nucleus in the basal cell portion, corresponding to *Sp-opsin4* RNA expression domain. [Scale bars, 100 μm (*A* and *B*) and 10 μm (*C*–*E*).]

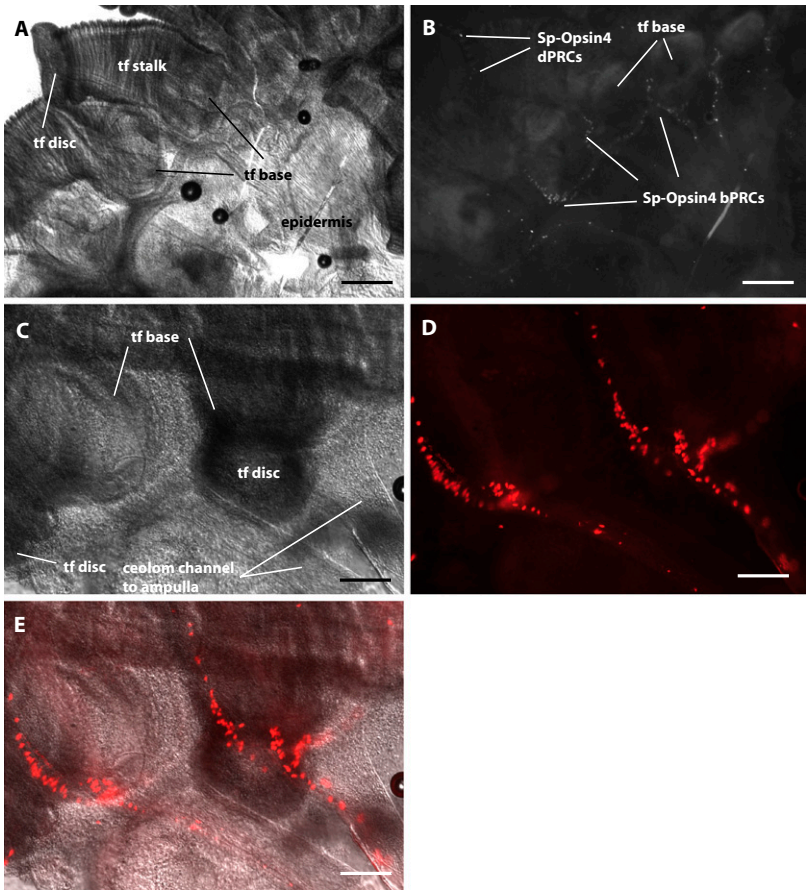

Fig. S3. (*A* and *B*) Top view on a *S. purpuratus* tube foot (tf) row dissected with parts of the skeleton, and subsequently decalcified. (*B*) Fluorescence picture of *A* showing antibody labeling against Sp-Opsin4 (white). Note that transmission of a small portion of bright field light allows for better orientation within the depicted tissue. (*C*–*E*) Another tissue section of the same specimen with inverted orientation, tube foot discs now facing downside. (*C*) Differential interference contrast picture of two tube feet. (*D*) Corresponding fluorescence picture of Sp-Opsin4 (red) immunoreactive PRCs. (*E*) Overlay of *C* and *D* depicting position of Sp-Opsin4–positive PRCs at the base of the two tube feet. [Scale bars, 200 μm (*A* and *B*) and 100 μm (*C*–*E*).]

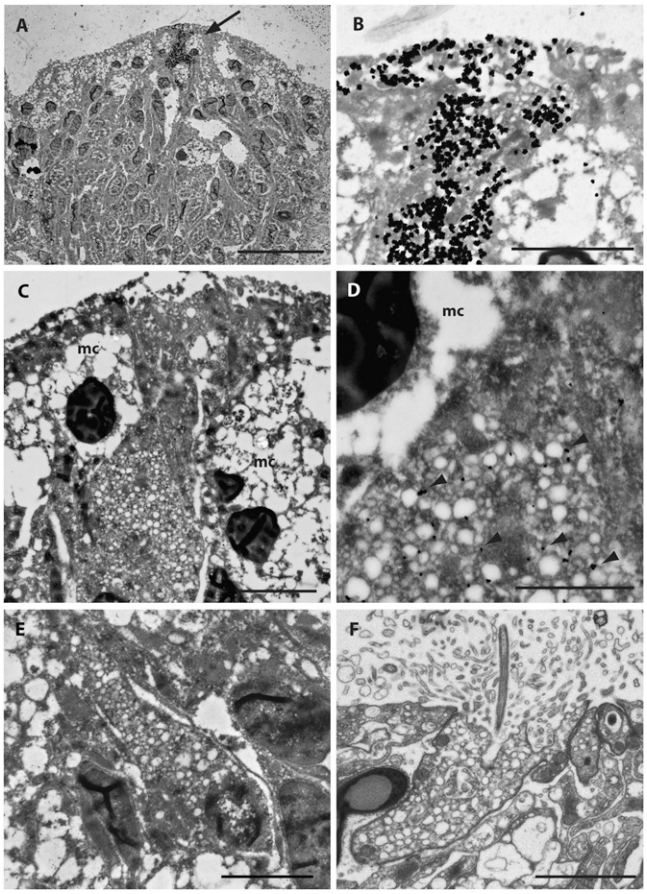

Fig. S4. Immunogold labeling of Sp-Opsin4 on TEM sections. (*A*–*E*) Trialdehyde fixation (0.5% glutaraldehyde/4% PFA in PBS), (*F*) glutaraldehyde fixation (2.5% glutaraldehyde in PBS). For details, see *SI Materials and Methods*. (*A*) Immunogold-labeled and gold-enhanced Sp-Opsin4–positive PRC in tube foot disk epidermis (arrowed). (*B*) Apical part of the same PRC showing strong labeling because of long enhancement time. (*C*) Different TEM section of the same specimen with immunogold labeling of Sp-Opsin4 but reduced gold enhancement (mc, mucus cell). (*D*) Partial magnification of *C* demonstrating specific labeling (arrowheads) of PRC and distinct cytoplasmatic PRC structure containing high numbers of vesicles. (*E*) Different TEM section of a PRC depicting immunogold labeling without gold enhancement. Colloidal gold labels not visible at this magnification. The section reported in *E*, compared with *F*, shows differences in tissue structure because of different fixation types. (*F*) Apical portion of PRC of another specimen fixed and processed for conventional TEM. [Scale bars, 10 μm (*A*), 2 μm (*B*, *C*, *E*, and *F*), and 1 μm (*D*).]

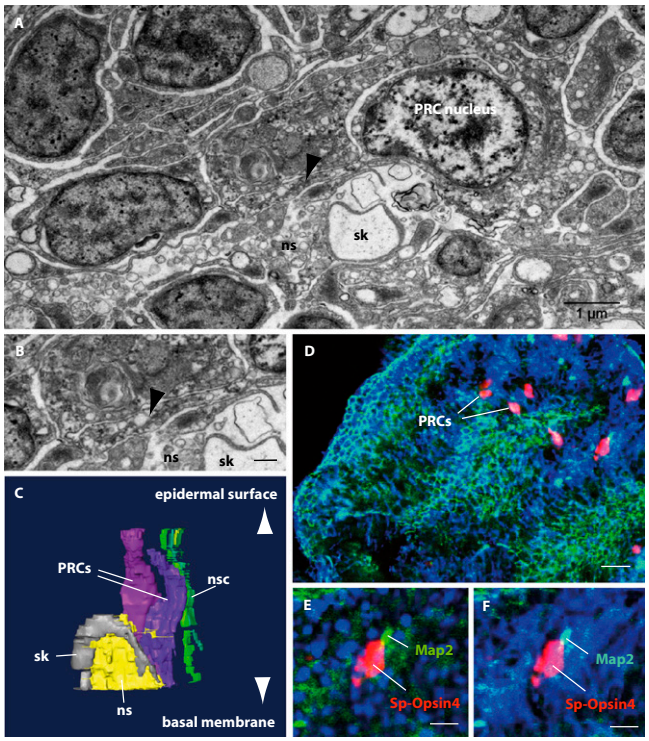

Fig. S5. Axonal and dendritic projections of the Sp-Opsin4–positive PRCs. (*A*) TEM section displaying axonal projection (black arrowhead) in the basal region of the PRC contacting the tube foot nervous system (ns, tube foot nervous system; sk, skeletal disk element). (*B*) Magnification of *A* showing detail of axon (black arrowhead). (*C*) Schematic reconstruction (Amira; 2.0) of TEM serial sections showing two PRCs running in close vicinity of the tube foot nervous system and a skeletal element. (nsc, neighboring sensory cells). (*D*) Triple antibody labeling against Sp-Opsin4 (red), Map2 (2a+2b; Sigma) (green/cyan) and acetylated-α-tubulin (purple) displaying net-like dendritic structures in the tube foot disk and in the apical portion of PRCs. (*E*) Magnification of *D* displaying nuclear staining instead of anti–acetylated-α-tubulin labeling. (*F*) Magnification of *D* showing clear Map2 labeling at the PRC apex (cyan). [Scale bars, 1 µm (*A* and *B*), 20 µm (*D*), and 10 µm (*E* and *F*).]